Scilight

Intelligence & Control
https://www.sciltp.com/journals/ic

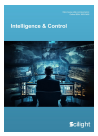

Article

Check for updates

Hopf Bifurcation and Stability Analysis of a Fractional-Order Lotka-Volterra Predator-Prey Model with Two Delays

Mengfan Zhu [1], Zunshui Cheng [1,*], Youming Xin [1], Yun Shang [1], Xue Lin [1] and Jinde Cao [2]

[1] School of Mathematics and Physics, Qingdao University of Science and Technology, Qingdao 266061, China
[2] School of Mathematics, Southeast University, Nanjing 211189, China
* Correspondence: chengzunshui@gmail.com

How To Cite: Zhu, M.; Cheng, Z.; Xin, Y.; et al. Hopf Bifurcation and Stability Analysis of a Fractional-Order Lotka-Volterra Predator-Prey Model with Two Delays. *Intelligence & Control* **2026**, *2*(2), 2. https://doi.org/10.53941/ic.2026.100005

Received: 21 January 2026
Revised: 11 April 2026
Accepted: 19 May 2026
Published: 16 June 2026

Abstract: This paper investigates the stability and Hopf bifurcation of a class of fractional-order Lotka-Volterra predator-prey models with two time delays. By selecting one time delay as the bifurcation parameter and fixing the other, the criterion for Hopf bifurcation induced by the corresponding time delay is derived. This paper also investigates the interaction between the two time delays via numerical simulations. The results show that the stability of the model can be either weakened or enhanced by appropriately adjusting the time delays. Finally, the feasibility of the proposed findings is verified through numerical examples.

Keywords: fractional-order; predator-prey system; time delays; hopf bifurcation; stability analysis

1. Introduction

The Lotka-Volterra predator-prey system is a classic model in mathematical biology, using equations to reveal the dynamic balance relationship between predator and prey populations in nature [1–8]. The Lotka-Volterra predator-prey model not only reveals the periodic fluctuation patterns between predators and prey, but is also widely applied in areas including biological resource management, pest control, and ecological stability assessment [9–11]. It provides important theoretical support for understanding community structure and guiding ecological conservation and sustainable utilization. Therefore, the dynamic behaviors of the Lotka-Volterra system have aroused great interest among scholars in various fields, and numerous research results have been achieved regarding its stability, persistence, periodic solutions, and bifurcation [12–16]. Xu et al. conducted the first systematic analysis of the case where the intrinsic growth rate vector $c \neq 0$ for the anti-symmetric Lotka-Volterra systems in [12]. Chen et al. investigated the stability of a Lotka-Volterra type predator-prey system with Allee effect in the predator and density-dependent birth rate in the prey, considering both the non-delayed and delayed cases in [13]. Xia et al. considered a symmetric Lotka-Volterra system and further analyzed the stability and direction of Hopf bifurcation by using the normal form method in [14]. A stochastic non-autonomous predator-prey model was investigated, and the existence of at least one positive periodic solution under certain simple and reasonable conditions was proved in [15]. Zhao et al. designed a controller for the Lotka-Volterra system and found that the critical value of time delay can be modified by tuning the control parameters in [16].

In real biological systems, multiple time delays are usually involved, such as delays in predator gestation, digestion, and resource regeneration. This implies that it is insufficient to only investigate the effect of a single time delay on biological models. Therefore, studying predator-prey models with multiple time delays can reflect real-world situations more accurately [17–19]. In particular, Xu et al. considered a model with two time delays in [20] based on the existing framework.

$$\begin{cases} \dot{x}(t) = x(t)[r_1 - a_{11}x(t-\tau_1) - a_{12}y(t-\tau_2)], \\ \dot{y}(t) = y(t)[-r_2 + a_{21}x(t-\tau_2) - a_{22}y(t-\tau_1)], \end{cases} \tag{1}$$

where $x(t)$ and $y(t)$ respectively represent the population densities of prey and predators at time t. $r_1 > 0$ represents the intrinsic growth rate of the prey, and $r_2 > 0$ represents the mortality rate of the predator. $a_{ij}(ij = 1, 2)$ are all positive constants. τ_1 is the gestation period of prey and predator. τ_2 is the hunting delay of predator to prey in the first equation of system (1). τ_2 is the feedback delay of the predator to the growth of the species itself in the second equation of system (1).

On the other hand, traditional integer-order differential equations are inherently limited in capturing memory, hereditary, and nonlocal characteristics, which are common in real biological systems. As an extension of integer-order differential equations, fractional-order systems introduce non-integer order differential operators and possess distinctive memory and hereditary properties [21–23]. They have been widely applied in various scientific and engineering fields, such as control engineering, neural networks, disease transmission, biological populations and image processing [24–29]. Ma et al. combined higher-order interactions with discrete fractional dynamics to construct a discrete fractional higher-order neural network model in [24]. The authors proposed the influence of fractional orders on the dynamical characteristics of the proposed fractional-order SIR model in [25]. Zhang et al. analyzed the bifurcation problem of a fractional-order disease spreading system in [26]. The authors upgraded the traditional model SISUV and SIRUV to a fractional-order system with Caputo-type fractional derivatives, accurately capturing the memory characteristics of disease transmission in [27]. Based on the GL fractional derivative, this paper achieved the optimization of edge detection for colour images in [29]. Compared with integer-order models, fractional-order predator-prey models can better describe realistic ecological scenarios, such as the cumulative effects of environmental factors during population growth and the memory effects in the growth of biological individuals. Therefore, fractional-order operators have been introduced into the predator-prey model [30–37]. For example, Mu and Xu et al. introduced the distributed delay and discrete delay into the original system and extended the system to the fractional-order case in [35]. The author considered a fractional prey–predator scavenger model as well as harvesting by a predator and scavenger in [36]. Li and Wang et al. adopted a time-delay feedback controller to regulate the stability of the fractional-order predator-prey system, achieving the desired effect and demonstrating strong practical application value in [37]. However, most existing studies on fractional-order Lotka-Volterra models focus on a single time delay.

Based on the above discussion, this paper investigates a fractional-order Lotka-Volterra predator-prey model with two time delays

$$\begin{cases} D^q x(t) = \alpha x(t)[r_1 - a_{11}x(t-\tau_1) - a_{12}y(t-\tau_2)] + \beta(x(t-\tau_1) - x^*), \\ D^q y(t) = \alpha y(t)[-r_2 + a_{21}x(t-\tau_2) - a_{22}y(t-\tau_1)] + \beta(y(t-\tau_1) - y^*), \end{cases} \tag{2}$$

where $q \in (0, 1]$ is the fractional order, $\alpha > 0$, $\beta \in \mathbb{R}$ are the control parameters, and (x^*, y^*) is the positive equilibrium point of system (1).

The main contributions of this paper are summarized as follows: (1) In contrast to previous studies, we extend the dual time-delay model to the fractional-order domain, which can describe the population dynamics more accurately. (2) This paper considers dual time delays, treats each of them as a bifurcation parameter, analyzes their effects on the system, and derives the corresponding bifurcation conditions. (3) Numerical simulations are performed to plot the stability switching curves, and the coupling effect between the two time delays is illustrated.

The rest of this paper is organized as follows. In Section 2, the relevant definitions of fractional derivatives are discussed. In Section 3, we discuss the existence and conditions of bifurcation. In Section 4, numerical examples are provided to verify the theoretical results. In Section 5, we provide a brief conclusion.

Notation. In this paper, $\mathbb{R}$ denotes the set of real numbers. $\mathbb{Z}^+$ denotes the the set of positive integers. $q \in (0, 1]$ is the fractional order. D^q represents the fractional-order derivative. $\Gamma(\cdot)$ stands for the Gamma function. $x(t), y(t)$ denote the state variables. $E(x^*, y^*)$ is the positive equilibrium point. τ_1, τ_2 represent the time delays. The critical value of τ_1 inducing Hopf bifurcation is expressed as τ_{1_0} and ω_0 is the corresponding critical frequency. The critical value of τ_2 inducing Hopf bifurcation is expressed as τ_{2_0} and $\bar{\omega}_0$ is the corresponding critical frequency.

2. Preliminaries

The common definitions of fractional derivatives include Riemann-Liouville derivative and Caputo derivative. In this section, the definition of Caputo fractional derivative is introduced to prepare for the subsequent work.

Definition 1 ([38]). *The definition of Caputo fractional-order derivative is denoted as*

$$D^q f(t) = \frac{1}{\Gamma(l-q)} \int_0^t (t-s)^{l-q-1} f^{(l)}(s)\, ds,$$

where $l-1 \le q < l$ *and* $l \in \mathbb{Z}^+$.

Definition 2 ([38]). *The Laplace transform of the Caputo fractional-order derivative is defined as*

$$L\{D^q f(t); s\} = s^q F(s) - \sum_{k=0}^{\iota-1} s^{q-k-1} f^{(k)}(0), \quad \iota - 1 \le q < \iota \in \mathbb{Z}^+.$$

If $f^{(k)}(0) = 0$, $k = 1, 2, \ldots, n$, *then* $L\{D^q f(t); s\} = s^q F(s)$.

3. Main Results

For the subsequent analysis, we first assume

H1. $r_1 a_{21} - r_2 a_{11} > 0$.

Under H1, we can calculate that system (2) has a unique positive equilibrium point $E(x^*, y^*)$, where

$$x^* = \frac{r_1 a_{22} + r_2 a_{12}}{a_{11} a_{22} + a_{12} a_{21}}, \quad y^* = \frac{r_1 a_{21} - r_2 a_{11}}{a_{11} a_{22} + a_{12} a_{21}}.$$

Let $u_1(t) = x(t) - x^*$, $u_2(t) = y(t) - y^*$, then system (2) becomes

$$\begin{cases} D^q u_1(t) = \alpha(u_1(t) + x^*)[r_1 - a_{11}(u_1(t-\tau_1) + x^*) \\ \qquad\qquad -a_{12}(u_2(t-\tau_2) + y^*)] + \beta u_1(t-\tau_1), \\ D^q u_2(t) = \alpha(u_2(t) + y^*)[-r_2 + a_{21}(u_1(t-\tau_2) + x^*) \\ \qquad\qquad -a_{22}(u_2(t-\tau_1) + y^*)] + \beta u_2(t-\tau_1). \end{cases} \tag{3}$$

Linearizing system (3), we obtain

$$\begin{cases} D^q u_1(t) = m_{11} u_1(t) + m_{12} u_1(t-\tau_1) + m_{13} u_2(t-\tau_2), \\ D^q u_2(t) = m_{21} u_2(t) + m_{22} u_1(t-\tau_2) + m_{23} u_2(t-\tau_1), \end{cases} \tag{4}$$

where

$$m_{11} = \alpha[r_1 - a_{11}x^* - a_{12}y^*],\ m_{12} = \beta - \alpha a_{11}x^*,\ m_{13} = -\alpha a_{12}x^*,$$
$$m_{21} = \alpha[-r_2 + a_{21}x^* - a_{22}y^*],\ m_{22} = \alpha a_{21}y^*,\ m_{23} = \beta - \alpha a_{22}y^*.$$

The characteristic equation of system (4) is

$$\det \begin{bmatrix} s^q - m_{11} - m_{12}e^{-s\tau_1} & -m_{13}e^{-s\tau_2} \\ \vdots & \vdots \\ -m_{22}e^{-s\tau_2} & s^q - m_{21} - m_{23}e^{-s\tau_1} \end{bmatrix} = 0. \tag{5}$$

By organizing and simplifying Equation (5), we have

$$\begin{aligned} s^{2q} - (m_{11} + m_{21})s^q + m_{11}m_{21} + [m_{23}(m_{11} - s^q) + m_{12}(m_{21} - s^q)]e^{-s\tau_1} \\ + m_{12}m_{23}e^{-2s\tau_1} - m_{13}m_{22}e^{-2s\tau_2} = 0. \end{aligned} \tag{6}$$

3.1. τ_1 Is Used as the Bifurcation Parameter

In this subsection, we first fix τ_2 and investigate the effect of τ_1 on bifurcation in system (2). Moreover, we provide the core theorem for determining the stability of the system equilibrium and the occurrence of Hopf bifurcation.

Theorem 1. *If system (2) satisfies the conditions H1–H5, then the following result holds*

(i) System (2) is locally asymptotically stable for $\tau_1 \in [0, \tau_{1_0})$.

(ii) System (2) is unstable when $\tau_1 > \tau_{1_0}$ *and it undergoes a Hopf bifurcation when* $\tau_1 = \tau_{1_0}$.

Where the assumptions are given as follows

H2. *ω is a common root of $f_1^2(\omega)+f_2^2(\omega)=1$ and $g_1^2(\omega)+g_2^2(\omega)=1$.*

H3. $\gamma_1>0$, $\gamma_2>0$.

H4. *Equation $\mathcal{Q}_1^2+\mathcal{Q}_2^2-\mathcal{P}_1^2-\mathcal{P}_2^2=0$ has no positive real root.*

H5. $Re[\frac{ds}{d\tau_1}]_{(\omega=\omega_0,\tau_1=\tau_{1_0})}\neq 0$, *where ω_0 is the critical frequency and τ_{1_0} is the bifurcation point.*

Subsequently, we perform key derivations to prove that Theorem 1 holds.
Equation (6) is rewritten as

$$P_1(s)+P_2(s)e^{-s\tau_1}+P_3(s)e^{-2s\tau_1}+P_4(s)e^{-2s\tau_2}=0, \tag{7}$$

where

$$\begin{aligned}
P_1(s)&=s^{2q}-(m_{11}+m_{21})s^q+m_{11}m_{21},\\
P_2(s)&=m_{11}m_{23}+m_{12}m_{21}-(m_{12}+m_{23})s^q,\\
p_3(s)&=m_{12}m_{23},\\
P_4(s)&=-m_{13}m_{22}.
\end{aligned}$$

Let $s=i\omega(\omega>0)$ be a purely imaginary root of Equation (7). Separating the real part and the imaginary part, we have

$$\begin{cases}
A_2cos(\omega\tau_1)+B_2sin(\omega\tau_1)+A_3cos(2\omega\tau_1)+B_3sin(2\omega\tau_1)\\
\qquad\qquad=-A_1-A_4cos(2\omega\tau_2)-B_4sin(2\omega\tau_2),\\
B_2cos(\omega\tau_1)-A_2sin(\omega\tau_1)+B_3cos(2\omega\tau_1)-A_3sin(2\omega\tau_1)\\
\qquad\qquad=-B_1-B_4cos(2\omega\tau_2)+A_4sin(2\omega\tau_2),
\end{cases} \tag{8}$$

where A_i, B_i are respectively the read and imaginary parts of $P_i(s)(i=1,2,3,4)$.
In accordance with the properties of trigonometric functions, Equation (8) becomes

$$k_1cos(\omega\tau_1)+k_2sin(\omega\tau_1)=k, \tag{9}$$

where

$$\begin{aligned}
k_1&=2(A_2A_3+B_2B_3),\ k_2=2(A_2A_3-B_2A_3),\\
k&=A_1^2+B_1^2-A_2^2-B_2^2-A_3^2-B_3^2+A_4^2+B_4^2\\
&\quad+2(A_1A_4+B_1B_4)cos(2\omega\tau_2)\\
&\quad+2(A_1B_4-B_1A_4)sin(2\omega\tau_2).
\end{aligned}$$

Due to $sin(\omega\tau_1)=\pm\sqrt{1-cos^2(\omega\tau_1)}$, we discuss the cases separately.
Case a $sin(\omega\tau_1)=\sqrt{1-cos^2(\omega\tau_1)}$, Equation (9) becomes

$$k_1cos(\omega\tau_1)+k_2\sqrt{1-cos^2(\omega\tau_1)}=k. \tag{10}$$

By Equation (10), it is easily obtained that

$$cos(\omega\tau_1)=f_1(\omega),\ sin(\omega\tau_1)=f_2(\omega).$$

Obviously,

$$f_1^2(\omega)+f_2^2(\omega)=1.$$

Thus, we have

$$\tau_{1_1}^{(k)}=\frac{1}{\omega}[arccosf_1(\omega)+2k\pi],\ k=0,1,2,\ldots.$$

Case b $sin(\omega\tau_1) = -\sqrt{1 - cos^2(\omega\tau_1)}$, Equation (9) becomes

$$k_1 cos(\omega\tau_1) - k_2\sqrt{1 - cos^2(\omega\tau_1)} = k. \tag{11}$$

By Equation (11), it is easily obtained that

$$cos(\omega\tau_1) = g_1(\omega),\ sin(\omega\tau_1) = g_2(\omega).$$

Obviously,

$$g_1^2(\omega) + g_2^2(\omega) = 1.$$

Thus, we have

$$\tau_{1_2}^{(k)} = \frac{1}{\omega}[arccosg_1(\omega) + 2k\pi],\ k = 0, 1, 2, \ldots.$$

Under the condition H2, the bifurcation point is defined as

$$\tau_{1_0} = min\{\tau_{1_1}^{(k)}, \tau_{1_2}^{(k)}\},\ k = 0, 1, 2, \ldots. \tag{12}$$

We analyze the stability for $\tau_1 = 0$, in which case the characteristic (7) becomes

$$\mathcal{P}(s) + \mathcal{Q}(s)e^{-2s\tau_2} = 0, \tag{13}$$

where

$$\mathcal{P} = s^{2q} - (m_{11} + m_{21} + m_{12} + m_{23})s^q + (m_{11} + m_{12})(m_{21} + m_{23}), \mathcal{Q} = -m_{13}m_{22}.$$

If $\tau_2 = 0$ and let $\lambda = s^q$, then Equation (13) becomes

$$\lambda^2 + \gamma_1\lambda + \gamma_2 = 0, \tag{14}$$

where

$$\gamma_1 = -(m_{11} + m_{12} + m_{21} + m_{23}),$$
$$\gamma_2 = (m_{11} + m_{12})(m_{21} + m_{23}) - m_{13}m_{22}.$$

Let $\mathcal{P} = \mathcal{P}_1 + i\mathcal{P}_2$, $\mathcal{Q} = \mathcal{Q}_1 + i\mathcal{Q}_2$, Equation (13) becomes

$$\mathcal{P}_1 + i\mathcal{P}_2 + (\mathcal{Q}_1 + i\mathcal{Q}_2)e^{-2s\tau_2} = 0. \tag{15}$$

Assume that $s = i\phi(\phi > 0)$ is a root of Equation (15). Separating the real part and imaginary part, we have

$$\begin{cases} \mathcal{Q}_1 cos(2\phi\tau_2) + \mathcal{Q}_2 sin(2\phi\tau_2) = -\mathcal{P}_1, \\ \mathcal{Q}_2 cos(2\phi\tau_2) - \mathcal{Q}_1 sin(2\phi\tau_2) = -\mathcal{P}_2, \end{cases}$$

then

$$\mathcal{Q}_1^2 + \mathcal{Q}_2^2 - \mathcal{P}_1^2 - \mathcal{P}_2^2 = 0. \tag{16}$$

It is readily seen from H3 that all characteristic roots of the characteristic Equation (14) have negative real parts. Combined with H4, we can directly draw the conclusion that the equilibrium point of the fractional-order Lotka-Volterra system (2) is locally asymptotically stable when $\tau_1 = 0$.

To prove the occurrence of Hopf bifurcation, it is necessary to verify the transversality condition, for which Lemma 1 is presented.

Lemma 1. *Assume that $s(\tau_1) = \zeta(\tau_1) + i\omega(\tau_1)$ is the root of Equation (7) near $\tau_1 = \tau_{1_0}$ and satisfies $\zeta(\tau_{1_0}) = 0$, $\omega(\tau_{1_0}) = \omega_0$, then the transversality condition holds*

$$Re\left[\frac{ds}{d\tau_1}\right]_{(\omega=\omega_0, \tau_1=\tau_{1_0})} \neq 0.$$

Proof. We differentiate Equation (6) with respect to τ_1, then

$$\begin{aligned}
&2qs^{2q-1}\frac{ds}{d\tau_1} - q(m_{11}+m_{21})s^{q-1}\frac{ds}{d\tau_1} + [-qm_{23}s^{q-1}\frac{ds}{d\tau_1} - qm_{12}s^{q-1}\frac{ds}{d\tau_1}]e^{-s\tau_1} \\
&+ [m_{23}(m_{11}-s^q) + m_{12}(m_{21}-s^q)][-se^{-s\tau_1} - \tau_1 e^{-s\tau_1}\frac{ds}{d\tau_1}] \\
&+ m_{12}m_{23}[-2se^{-2s\tau_1} - 2\tau_1 e^{-2s\tau_1}\frac{ds}{d\tau_1}] + 2m_{13}m_{22}\tau_2 e^{-2s\tau_2}\frac{ds}{d\tau_1} = 0.
\end{aligned}$$

We obtain

$$\frac{ds}{d\tau_1} = \frac{\eta(s)}{\theta(s)}, \tag{17}$$

where

$$\begin{aligned}
\eta(s) &= [m_{23}(m_{11}-s^q) + m_{12}(m_{21}-s^q)]se^{-s\tau_1} + 2m_{12}m_{23}se^{-2s\tau_1}, \\
\theta(s) &= 2qs^{2q-1} - q(m_{11}+m_{21})s^{q-1} - q(m_{12}+m_{23})s^{q-1}e^{-s\tau_1} - \tau_1[m_{23}(m_{11}-s^q) \\
&\quad + m_{12}(m_{21}-s^q)]e^{-s\tau_1} - 2m_{12}m_{23}\tau_1 e^{-2s\tau_1} + 2m_{13}m_{23}\tau_2 e^{-2s\tau_2}.
\end{aligned}$$

From Equation (17), the result is yielded

$$Re\left[\frac{ds}{d\tau_1}\right]_{(\omega=\omega_0,\tau_1=\tau_{1_0})} = \frac{\eta_1\theta_1 + \eta_2\theta_2}{\theta_1^2+\theta_2^2}, \tag{18}$$

where η_1, η_2 are respectively the real and imaginary parts of $\eta(s)$. θ_1, θ_2 are respectively the real and imaginary parts of $\theta(s)$. The expressions of η_1, η_2, θ_1, θ_2 are provided in Appendix A.

According to the assumption H5, we can deduce that transversality condition hold. This completes the proof of Lemma 1. □

3.2. τ_2 Is Used as the Bifurcation Parameter

In this subsection, we fix τ_1 and investigate the influence of τ_2 on bifurcation in system (2), and establish the following theorem for stability and Hopf bifurcation.

Theorem 2. *If system (2) satisfies the conditions H1 and H6–H9, then the following result holds*

(i) *System (2) is locally asymptotically stable for $\tau_2 \in [0, \tau_{2_0})$.*

(ii) *System (2) is unstable when $\tau_2 > \tau_{2_0}$ and it undergoes a Hopf bifurcation when $\tau_2 = \tau_{2_0}$.*

Where the assumptions are given as follows

H6. *Equation $H_1^2(\bar{\omega}) + H_2^2(\bar{\omega}) = 1$ has at least one positive real root.*

H7. $\zeta_1 > 0, \zeta_2 > 0$.

H8. *Equation $Y_1^2(\psi) + Y_2^2(\psi) = 1$ has no positive real root.*

H9. $Re[\frac{ds}{d\tau_2}]_{(\bar{\omega}=\bar{\omega}_0,\tau_2=\tau_{2_0})} \neq 0$, *where $\bar{\omega}_0$ is the critical frequency and τ_{2_0} is the bifurcation point.*

Similarly, we perform key derivations to prove that Theorem 2 holds.

Let $s = i\bar{\omega}(\bar{\omega} > 0)$ be a purely imaginary root of Equation (7). Separating the real and imaginary parts yields

$$\begin{cases}
-A_4cos(2\bar{\omega}\tau_2) - B_4sin(2\bar{\omega}\tau_2) = & A_1 + A_2cos(\bar{\omega}\tau_1) + B_2sin(\bar{\omega}\tau_1) \\
& +A_3cos(2\bar{\omega}\tau_1) + B_3sin(2\bar{\omega}\tau_1), \\
-B_4cos(2\bar{\omega}\tau_2) + A_4sin(2\bar{\omega}\tau_2) = & B_1 + B_2cos(\bar{\omega}\tau_1) - A_2sin(\bar{\omega}\tau_1) \\
& +B_3cos(2\bar{\omega}\tau_1) - A_3sin(2\bar{\omega}\tau_1),
\end{cases} \tag{19}$$

where A_i, B_i $(i = 1, 2, 3, 4)$ are consistent with the above .

Solving the Equation (19), we can obtain

$$\begin{cases} cos(2\bar{\omega}\tau_2) = \frac{-A_4h_1+B_4h_2}{A_4^2+B_4^2} = H_1(\bar{\omega}), \\ sin(2\bar{\omega}\tau_2) = \frac{B_4h_1+A_4h_2}{A_4^2+B_4^2} = H_2(\bar{\omega}), \end{cases} \tag{20}$$

where

$$h_1 = A_1 + A_2cos(\bar{\omega}\tau_1) + B_2sin(\bar{\omega}\tau_1) + A_3cos(2\bar{\omega}\tau_1) + B_3sin(2\bar{\omega}\tau_1),$$
$$h_2 = B_1 + B_2cos(\bar{\omega}\tau_1) - A_2sin(\bar{\omega}\tau_1) + B_3cos(2\bar{\omega}\tau_1) - A_3sin(2\bar{\omega}\tau_1).$$

Obviously,

$$H_1^2(\bar{\omega}) + H_2^2(\bar{\omega}) = 1. \tag{21}$$

It follows from the first equation of Equation (20) that

$$\tau_2^{(k)} = \frac{1}{2\bar{\omega}}[arccosH_1(\bar{\omega}) + 2k\pi],\ k = 0, 1, 2, \ldots.$$

Under the condition (H6), the bifurcation point is defined as

$$\tau_{2_0} = min\{\tau_2^{(k)}\},\ k = 0, 1, 2, \ldots. \tag{22}$$

We analyze the stability for $\tau_2 = 0$, in which case the characteristic Equation (7) becomes

$$T_1(s) + T_2(s)e^{-s\tau_1} + T_3(s)e^{-2s\tau_1} = 0, \tag{23}$$

where

$$T_1(s) = s^{2q} - (m_{11} + m_{21})s^q + m_{11}m_{21} - m_{13}m_{22},$$
$$T_2(s) = m_{11}m_{23} + m_{12}m_{21} - (m_{12} + m_{23})s^q,$$
$$T_3(s) = m_{12}m_{23}.$$

If $\tau_1 = 0$ and let $\lambda = s^q$, then Equation (23) becomes

$$\lambda^2 + \zeta_1\lambda + \zeta_2 = 0, \tag{24}$$

where

$$\zeta_1 = -(m_{11} + m_{12} + m_{21} + m_{23}),$$
$$\zeta_2 = (m_{11} + m_{12})(m_{21} + m_{23}) - m_{13}m_{22}.$$

Then, we multiply both sides of Equation (23) by $e^{s\tau_1}$

$$T_1(s)e^{s\tau_1} + T_2(s) + T_3(s)e^{-s\tau_1} = 0. \tag{25}$$

Assume that $s = i\psi(\psi > 0)$ is a root of Equation (25) and $T_1(s) = E_1 + iF_1$, $T_2(s) = E_2 + iF_2$, $T_3(s) = E_3 + iF_3$, we can get

$$\begin{cases} (E_1 + E_3)cos(\psi\tau_1) + (F_3 - F_1)sin(\psi\tau_1) = -E_2, \\ (F_3 + F_1)cos(\psi\tau_1) + (E_1 - E_3)sin(\psi\tau_1) = -F_2. \end{cases} \tag{26}$$

From Equation (26), we have

$$\begin{cases} cos(\psi\tau_1) = \frac{-E_2(E_1-E_3)+F_2(F_3-F_1)}{E_1^2+F_1^2-E_3^2-F_3^2} = Y_1(\psi), \\ sin(\psi\tau_1) = \frac{-F_2(E_1+E_3)+E_2(F_3+F_1)}{E_1^2+F_1^2-E_3^2-F_3^2} = Y_2(\psi). \end{cases} \tag{27}$$

Clearly,

$$Y_1^2(\psi) + Y_2^2(\psi) = 1. \tag{28}$$

It is readily seen from (H7) that all characteristic roots of the characteristic Equation (24) have negative real parts. Combined with (H8), we can directly draw the conclusion that the equilibrium point of the fractional-order Lotka-Volterra system (2) is locally asymptotically stable when $\tau_2 = 0$.

To ensure the occurrence of Hopf bifurcation, the transversality condition must be verified, as given in Lemma 2.

Lemma 2. *Assume that $s(\tau_2) = \zeta(\tau_2) + i\bar{\omega}(\tau_2)$ is the root of Equation (8) near $\tau_2 = \tau_{2_0}$ and satisfies $\zeta(\tau_{2_0}) = 0$, $\bar{\omega}(\tau_{2_0}) = \bar{\omega}_0$, then the transversality condition holds*

$$Re\left[\frac{ds}{d\tau_2}\right]_{(\bar{\omega}=\bar{\omega}_0,\tau_2=\tau_{2_0})} \neq 0.$$

Proof. We take the derivative of Equation (6) with respect to τ_2, then

$$\begin{aligned}
&2qs^{2q-1}\frac{ds}{d\tau_2} - q(m_{11}+m_{21})s^{q-1}\frac{ds}{d\tau_2} + [-qm_{23}s^{q-1}\frac{ds}{d\tau_2} - qm_{12}s^{q-1}\frac{ds}{d\tau_2}]e^{-s\tau_1} \\
&- \tau_1[m_{23}(m_{11}-s^q) + m_{12}(m_{21}-s^q)]e^{-s\tau_1}\frac{ds}{d\tau_2} - 2\tau_1 m_{12}m_{23}e^{-2s\tau_1}\frac{ds}{d\tau_2} \\
&- m_{13}m_{22}[-2se^{-2s\tau_2} - 2\tau_2 e^{-2s\tau_2}\frac{ds}{d\tau_2}] = 0.
\end{aligned}$$

We have

$$\frac{ds}{d\tau_2} = \frac{\rho(s)}{\sigma(s)}, \tag{29}$$

where

$$\begin{aligned}
\rho(s) &= -2sm_{13}m_{22}e^{-2s\tau_2}, \\
\sigma(s) &= 2qs^{2q-1} - q(m_{11}+m_{21})s^{q-1} - qs^{q-1}(m_{23}+m_{12}e^{-s\tau_1}) \\
&\quad - \tau_1[m_{23}(m_{11}-s^q) + m_{12}(m_{21}-s^q)]e^{-s\tau_1} \\
&\quad - 2\tau_1 m_{12}m_{23}e^{-2s\tau_1} + 2\tau_2(m_{13}m_{22})e^{-2s\tau_2}.
\end{aligned}$$

By Equation (29), we obtain

$$Re\left[\frac{ds}{d\tau_2}\right]_{(\bar{\omega}=\bar{\omega}_0,\tau_2=\tau_{2_0})} = \frac{\rho_1\sigma_1 + \rho_2\sigma_2}{\sigma_1^2 + \sigma_2^2}, \tag{30}$$

where ρ_1, ρ_2 are respectively the real and imaginary parts of $\rho(s)$. σ_1, σ_2 are respectively the real and imaginary parts of $\sigma(s)$. And the ρ_1, ρ_2, σ_1, σ_2 are provided in Appendix B.

As a result, the assumption (H9) implies that the transversality condition holds. This completes the proof of Lemma 2. □

Remark 1. *According to the Definition 1, when $q = 1$, the fractional-order model reduces to an integer order model. Therefor, the conclusions obtained below are still valid for the integer-order system.*

Remark 2. *Since system (1) and system (2) have the same unique positive equilibrium, we denote them uniformly as $E(x^*, y^*)$.*

Remark 3. *Equations (14) and (24) have the same expression*

$$\lambda^2 - (m_{11}+m_{12}+m_{21}+m_{23})\lambda + [(m_{11}+m_{12})(m_{21}+m_{23}) - m_{13}m_{22}] = 0.$$

According to the Routh-Hurwitz stability criterion, system (2) is asymptotically stable if and only if all roots of the above equations have negative real parts.

4. Numerical Simulations

To verify the validity of the theoretical results, we select the following fractional-order predator-prey model with two time delays for numerical simulation

$$\begin{cases}
D^{0.97}x(t) = x(t)[0.5 - 0.5x(t-\tau_1) - y(t-\tau_2)] + 0.1(x(t-\tau_1) - x^*), \\
D^{0.97}y(t) = y(t)[-0.5 + x(t-\tau_2) - y(t-\tau_1)] + 0.1(y(t-\tau_1) - y^*),
\end{cases} \tag{31}$$

where $q = 0.97$, $\alpha = 1$, $\beta = 0.1$, $r_1 = 0.5$, $r_2 = 0.5$, $a_{11} = 0.5$, $a_{12} = 1$, $a_{21} = 1$, $a_{22} = 1$.

Since (H1) holds, system (31) has a unique positive equilibrium point $E^*(\frac{2}{3}, \frac{1}{6})$.

4.1. τ_1 as the Bifurcation Parameter

Selecting $\tau_2 = 1.5$, we obtain critical frequency $\omega_0 = 0.32896$ and critical value $\tau_{1_0} = 1.171$. It is easy to calculate that (H2) and (H5) holds. The equilibrium point E^* of system (31) is stable when $\tau_1 = 0.8 < \tau_{1_0}$, which is simulated in Figure 1. The system loses stability, accompanied by a bifurcation when $\tau_1 = 1.5 > \tau_{1_0}$, as shown in Figure 2. Figure 3 shows that, within the considered region [0.6,1.8], as τ_2 increase (decrease), the critical value τ_{1_0} decreases (increases) monotonically. This implies that the the system undergoes Hopf bifurcation at a smaller (larger) value of τ_1, meaning that the bifurcation occurs earlier (later). Figure 4 further verifies this conclusion.

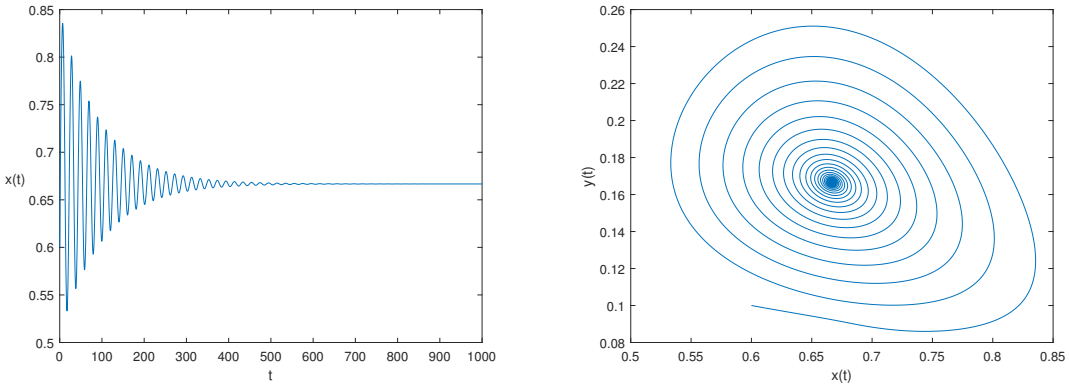

Figure 1. The trajectory and portrait diagram of system (31) with $\tau_2 = 1.5$, $\tau_1 = 0.8 < \tau_{1_0} = 1.171$.

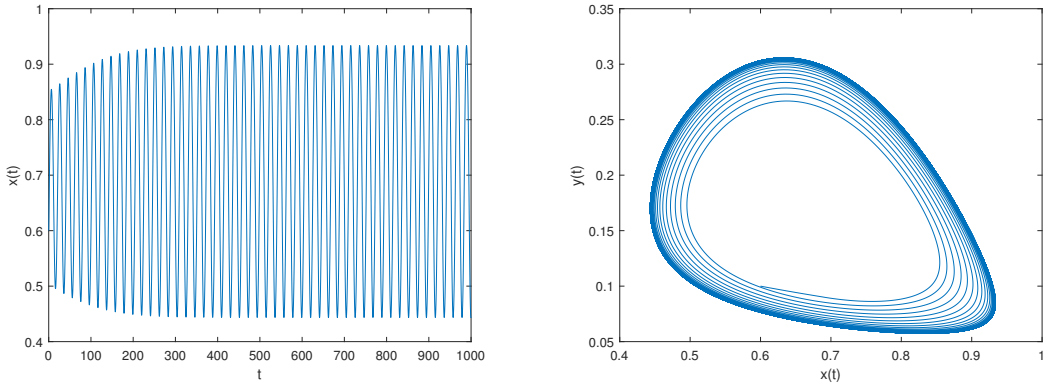

Figure 2. The trajectory and portrait diagram of system (31) with $\tau_2 = 1.5$, $\tau_1 = 1.5 > \tau_{1_0} = 1.171$.

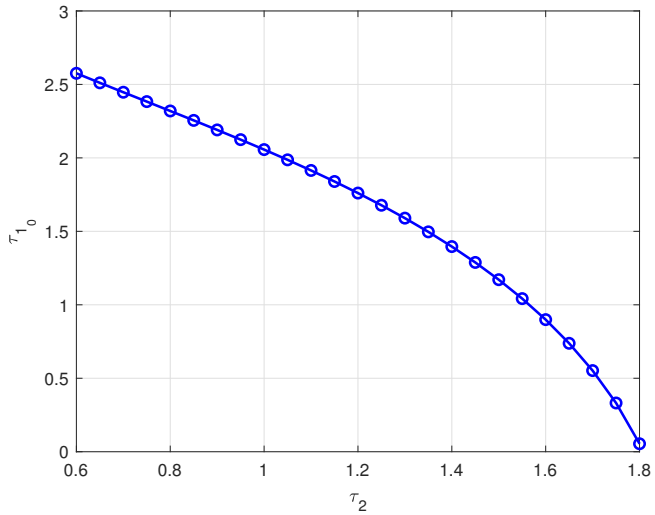

Figure 3. The value of τ_{1_0} relying on τ_2 in system (31).

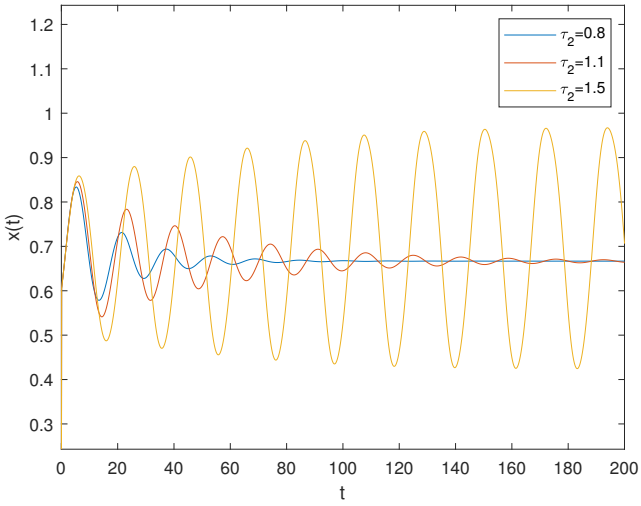

Figure 4. The trajectory of system (31) with $\tau_1 = 1.6$ for different τ_2.

4.2. τ_2 as the Bifurcation Parameter

We select $\tau_1 = 2$, then $\omega_0 = 0.39768$, $\tau_{2_0} = 1.0406$. And assumptions (H7) and (H9) holds. The equilibrium point E^* of system (31) is stable when $\tau_2 = 0.8 < \tau_{2_0}$, which is illustrated in Figure 5. The system is unstable and undergoes a bifurcation when $\tau_2 = 1.2 > \tau_{2_0}$, as shown in Figure 6. Figure 7 shows that, within the considered region [1,2], as τ_1 increase (decrease), the critical value τ_{2_0} decreases (increases) monotonically. This implies that the the system undergoes Hopf bifurcation at a smaller (larger) value of τ_2, meaning that the bifurcation occurs earlier (later). Figure 8 further verifies this conclusion. The switching curves are shown in Figure 9. These curves are composed of numerous critical points (τ_{1_0}, τ_{2_0}) and exhibit a multi-branch structure.

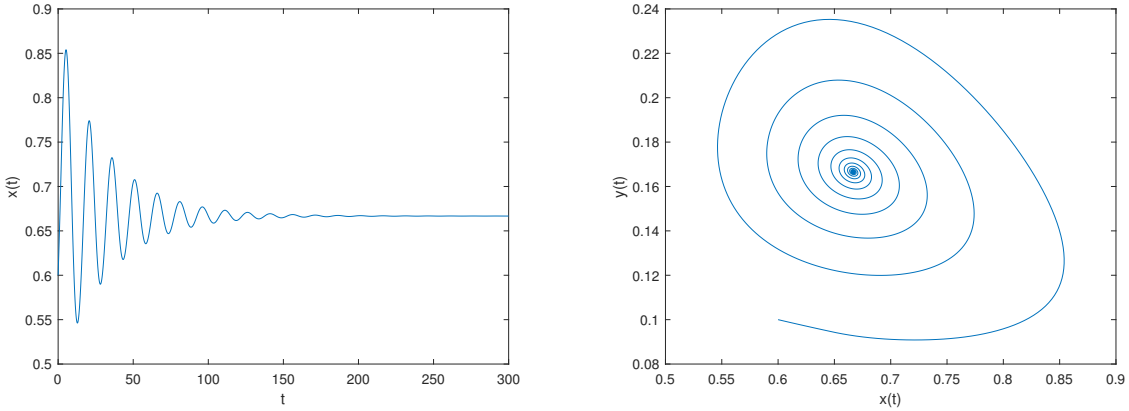

Figure 5. The trajectory and portrait diagram of system (31) with $\tau_1 = 2$, $\tau_2 = 0.8 < \tau_{2_0} = 1.0406$.

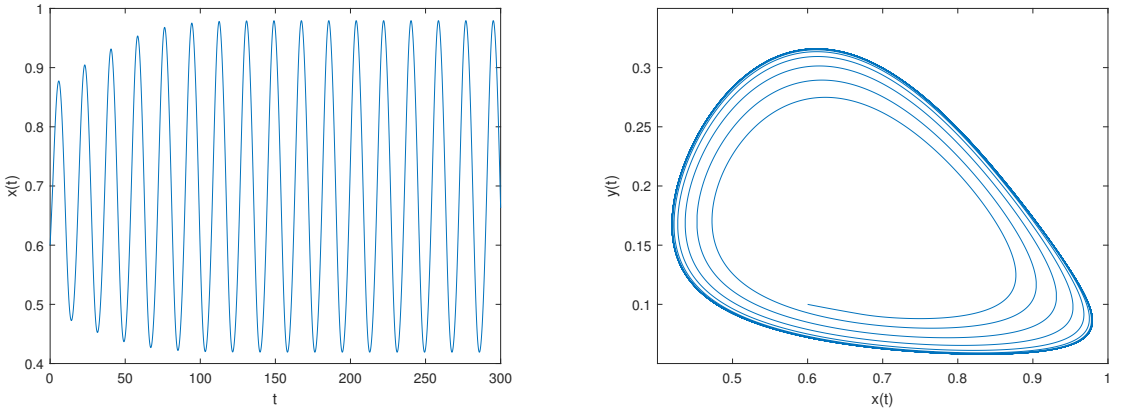

Figure 6. The trajectory and portrait diagram of system (31) with $\tau_1 = 2$, $\tau_2 = 1.2 > \tau_{2_0} = 1.0406$.

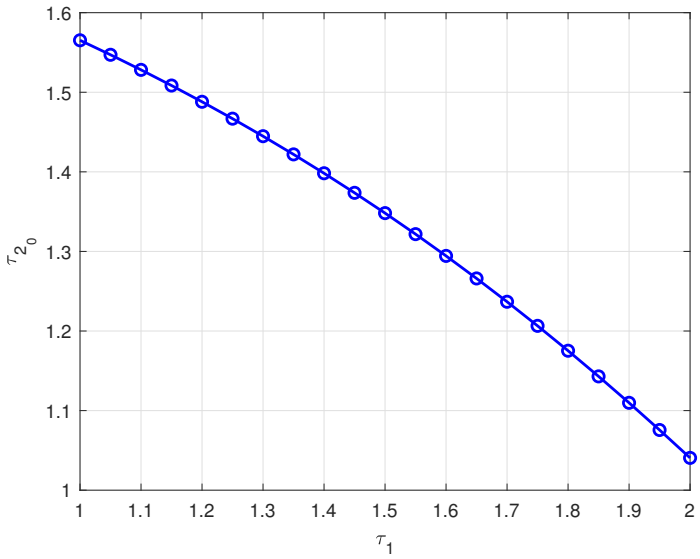

Figure 7. The value of τ_{2_0} relying on τ_1 in system (31).

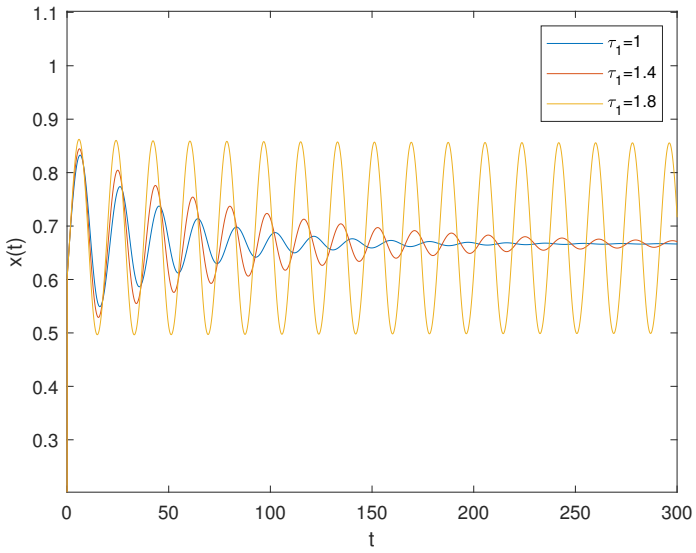

Figure 8. The trajectory of system (31) with $\tau_2 = 1.3$ for different τ_1.

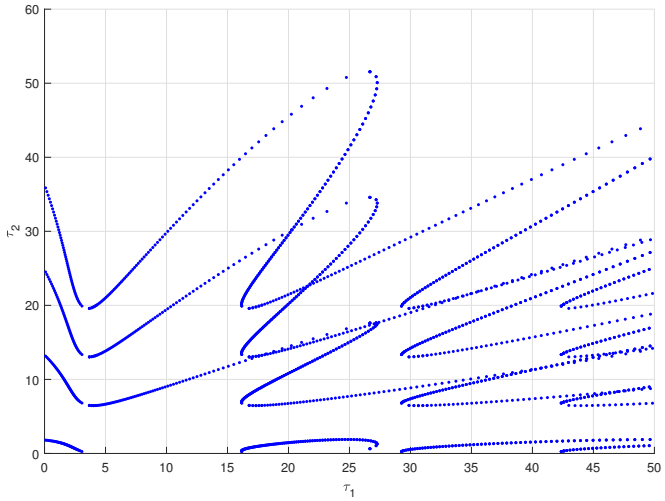

Figure 9. Plot of stability switching curves when $\tau_1 > 0, \tau_2 > 0$.

5. Conclusions

In this paper, we have analyzed the bifurcation behaviors of a fractional-order Lotka-Volterra predator–prey model with two delays. It is found that the proposed fractional-order system exhibits favorable stability when the time delay (chosen as the bifurcation parameter) is relatively small. Once it exceeds the critical value, the system loses stability and undergoes Hopf bifurcation. Furthermore, numerical simulations in this paper demonstrate that increasing (decreasing) either time delay will decrease (increase) the bifurcation critical value corresponding to the other delay, thereby weakening (enhancing) the stability of the proposed fractional-order model. In future research work, there are still some interesting and important issues worthy of further exploration, for instance, how to use system parameters or fractional order as bifurcation parameters to analyze the bifurcation problems of fractional-order Lotka-Volterra predator-prey models with different delays. These research topics are more challenging.

Appendix A

Derivation of θ_1, θ_2, η_1, η_2 in Equation (18).

$$\begin{aligned}
\theta_1(s) =&\omega_0(m_{23}m_{11}+m_{12}m_{21}sin(\omega_0\tau_{1_0}))-\omega_0^{q+1}(m_{23}+m_{21})cos(\frac{q+1}{2}\pi-\omega_0\tau_{1_0})\\
&+2\omega_0m_{12}m_{23}sin(2\omega_0\tau_{1_0}),\\
\theta_2(s) =&\omega_0(m_{23}m_{11}+m_{12}m_{21}cos(\omega_0\tau_{1_0}))-\omega_0^{q+1}(m_{23}+m_{21})sin(\frac{q+1}{2}\pi-\omega_0\tau_{1_0})\\
&+2\omega_0m_{12}m_{23}cos(2\omega_0\tau_{1_0}),\\
\eta_1(s) =&2q\omega_0^{2q-1}cos(\frac{2q-1}{2}\pi)-q\omega_0^{q-1}(m_{11}+m_{21})cos(\frac{q-1}{2}\pi)\\
&-q\omega_0^{q-1}(m_{12}+m_{23})cos(\frac{q-1}{2}\pi-\omega_0\tau_{1_0})-\tau_{1_0}(m_{23}m_{11}+m_{12}m_{21})cos(\omega_0\tau_{1_0})\\
&+\tau_{1_0}\omega_0^q(m_{23}+m_{12})cos(\frac{q}{2}\pi-\omega_0\tau_{1_0})-2\tau_{1_0}m_{12}m_{23}cos(2\omega_0\tau_{1_0})+2\tau_2m_{13}m_{22}cos(2\omega_0\tau_2),\\
\eta_2(s) =&2q\omega_0^{2q-1}sin(\frac{2q-1}{2}\pi)-q\omega_0^{q-1}(m_{11}+m_{21})sin(\frac{q-1}{2}\pi)\\
&-q\omega_0^{q-1}(m_{12}+m_{23})sin(\frac{q-1}{2}\pi-\omega_0\tau_{1_0})+\tau_{1_0}(m_{23}m_{11}+m_{12}m_{21})sin(\omega_0\tau_{1_0})\\
&+\tau_{1_0}\omega_0^q(m_{23}+m_{12})sin(\frac{q}{2}\pi-\omega_0\tau_{1_0})+2\tau_{1_0}m_{12}m_{23}sin(2\omega_0\tau_{1_0})-2\tau_2m_{13}m_{22}sin(2\omega_0\tau_2).
\end{aligned}$$

Appendix B

Derivation of ρ_1, ρ_2, σ_1, σ_2 in Equation (30)

$$\begin{aligned}
\rho_1 =&-2\bar{\omega}_0m_{13}m_{22}sin(2\bar{\omega}_0\tau_{2_0}),\\
\rho_2 =&-2\bar{\omega}_0m_{13}m_{22}cos(2\bar{\omega}_0\tau_{2_0}),\\
\sigma_1 =&2q\bar{\omega}_0^{2q-1}cos(\frac{2q-1}{2}\pi)-q\bar{\omega}_0^{q-1}(m_{11}+m_{21})cos(\frac{q-1}{2}\pi)\\
&-q\bar{\omega}_0^{q-1}(m_{12}+m_{23})cos(\frac{q-1}{2}\pi-\bar{\omega}_0\tau_1)-\tau_1(m_{23}m_{11}+m_{12}m_{21})cos(\bar{\omega}_0\tau_1)\\
&+\tau_1\bar{\omega}_0^q(m_{23}+m_{12})cos(\frac{q}{2}\pi-\bar{\omega}_0\tau_1)-2\tau_1m_{12}m_{23}cos(2\bar{\omega}_0\tau_1)+2\tau_{2_0}m_{13}m_{22}cos(2\bar{\omega}_0\tau_{2_0}),\\
\sigma_2 =&2q\bar{\omega}_0^{2q-1}sin(\frac{2q-1}{2}\pi)-q\bar{\omega}_0^{q-1}(m_{11}+m_{21})sin(\frac{q-1}{2}\pi)\\
&-q\bar{\omega}_0^{q-1}(m_{12}+m_{23})sin(\frac{q-1}{2}\pi-\bar{\omega}_0\tau_1)+\tau_1(m_{23}m_{11}+m_{12}m_{21})sin(\bar{\omega}_0\tau_1)\\
&+\tau_1\bar{\omega}_0^q(m_{23}+m_{12})sin(\frac{q}{2}\pi-\bar{\omega}_0\tau_1)+2\tau_1m_{12}m_{23}sin(2\bar{\omega}_0\tau_1)-2\tau_{2_0}m_{13}m_{22}sin(2\bar{\omega}_0\tau_{2_0}).
\end{aligned}$$

Author Contributions

M.Z.: Method design, Data analysis, Manuscirpt drafting; Z.C.: Writing—review & editing, Supervision, Methodology; Y.X.: data curation; Y.S.: Manuscirpt revision; X.L.: data analysis; J.C.: Manuscirpt revision. All authors have read and agreed to the published version of the manuscript.

Funding:

This work was supported by National Natural Science Foundation of China (Grant Nos. 61374011, 62103215, 62103217), Natural Science Foundation of Shandong Province of China (Grant Nos. ZR2020MF080, ZR2024MF040), and QUST (Grant Nos. 2024YKC06, 2023YJG08).

Institutional Review Board Statement

Not applicable.

Informed Consent Statement

Not applicable.

Data Availability Statement:

Data are contained within the article.

Conflicts of Interest:

The authors declare no conflict of interest. The funders had no role in the design of the study; in the collection, analyses, or interpretation of data; in the writing of the manuscript; or in the decision to publish the results.

Use of AI and AI-Assisted Technologies

No AI tools were utilized for this paper.

References

1. Zu, L.; Jiang, D.; O'Regan, D.; et al. Ergodic property of a Lotka-Volterra predator-prey model with white noise higher order perturbation under regime switching. *Appl. Math. Comput.* **2018**, *330*, 93–102.
2. Costa, M.A.V.; Morales-Rodrigo, C.; Suarez, A. Lotka-Voterra competition model with nonlocal coefficient diffusion. *J. Differ. Equ.* **2025**, *439*, 113397.
3. Ma, Z.; Chen, F.; Wu, C.; et al. Dynamic behaviors of a Lotka-Volterra predator-prey model incorporating a prey refuge and predator mutual interference. *Appl. Math. Comput.* **2013**, *219*, 7945–7953.
4. Huang, Y.; Li, F.; Shi, J. Stability of synchronized steady state solution of diffusive Lotka-Volterra predator-prey model. *Appl. Math. Lett.* **2020**, *105*, 106331.
5. Jafari, S.; Bayani, A.; Rajagopal, K.; et al. The simplest chaotic Lotka-Volterra system with reflection, rotation, and inversion symmetries. *Chaos Solit. Fractal.* **2025**, *201*, 117305.
6. Yan, S.; Du, Z. Hopf bifurcation in a Lotka-Volterra competition-diffusion-advection model with time delay. *J. Differ. Equ.* **2023**, *344*, 74–101.
7. Pan, S. Asymptotic spreading in a Lotka-Volterra predator-prey system. *J. Math. Anal. Appl.* **2013**, *407*, 230–236.
8. Xu, C.; Wu, Y.; Lu, L. Permanence and global attractivity in a discrete Lotka-Volterra predator-prey model with delays. *Adv. Differ. Equ.* **2014**, *2014*, 208.
9. Nie, L.; Teng, Z.; Hu, L.; et al. The dynamics of a Lotka-Volterra predator-prey model with state dependent impulsive harvest for predator. *Biosystems* **2009**, *98*, 67–72.
10. Liu, B.; Zhang, Y.; Chen, L. The dynamical behaviors of a Lotk-Volterra predator-prey model concerning integrated pest management. *Nonlinear Anal. Real World Appl.* **2005**, *6*, 227–243.
11. Mao, R.; Su, Z.; Ma, X.; et al. An ecological population study of lampreys in the Lotka-Volterra tertiary trophic level based on sex differences. *Ecol. Modell.* **2024**, *496*, 110826.
12. Xu, M.; Liu, S.; Lou, Y. Persistence and extinction in the anti-symmetric Lotka-Volterra systems. *J. Differ. Equ.* **2024**, *387*, 299–323.
13. Chen, F.; Guan, X.; Huang, X.; et al. Dynamic behaviors of a Lotka-Volterra type predator-prey system with Allee effect on the predator species and density dependent birth rate on the prey species. *Open Math.* **2019**, *17*, 1186–1202.
14. Xia, J.; Yu, Z.; Yuan, R. Stability and Hopf bifurcation in a symmetric Lotka-Volterra predator-prey system with delays. *Electron. J. Differ. Equ.* **2013**, *2013*, 1–16.
15. Zu, L.; Jiang, D.; O'Regan, D.; et al. Periodic solution for a non-autonomous Lotka-Volterra predator-prey model with random perturbation. *J. Math. Anal. Appl.* **2015**, *430*, 428–437.
16. Zhao, H.; Sun, Y.; Wang, Z. Control of Hopf Bifurcation and Chaos in a Delayed Lotka-Volterra Predator-Prey System with Time-Delayed Feedbacks. *Abstr. Appl. Anal.* **2014**, *2014*, 104156.
17. Liang, Z.; Meng, X. Stability and Hopf bifurcation of a multiple delayed predator-prey system with fear effect, prey refuge and Crowley-Martin function. *Chaos Solit. Fractal.* **2023**, *175*, 113955.

18. Wang, S.; Tang, H.; Ma, Z. Hopf bifurcation of a multiple-delayed predator–prey system with habitat complexity. *Math. Comput. Simul.* **2021**, *180*, 1–23.
19. Zhang, Z.; Yang, H. Stability and bifurcation in a stage-structured predator-prey system with Holling-II functional response and multiple delays. *Int. J. Comput. Math.* **2015**, *92*, 542–561.
20. Xu, C.; Liao, M.; He, X. Stability and Hopf bifurcation analysis for a Lotka-Volterra predator-prey model with two delays. *Int. J. Appl. Math. Comput. Sci.* **2011**, *21*, 97–107.
21. Cui, X.; Xue, D.; Pan, F. Dynamic analysis and optimal control for a fractional-order delayed SIR epidemic model with saturated treatment. *Eur. Phys. J. Plus* **2022**, *137*, 586.
22. Wang, Z.; Huang, X.; Zhou, J. A numerical method for delayed fractional-order differential equations: Based on GL definition. *Appl. Math. Inf. Sci.* **2013**, *7*, 525–529.
23. Fan, Y.; Huang, X.; Wang, Z.; et al. Global Mittag-Leffler synchronization of delayed fractional-order memristive neural networks. *Adv. Differ. Equ.* **2018**, *2018*, 338.
24. Ma, W.; Ma, C.; Wang, X.; et al. Delayed control-based controllability of discrete fractional higher-order neural networks. *Chaos Solit. Fractal.* **2025**, *200*, 116933.
25. Koziol, K.; Stanislawski, R.; Bialic, G. Fractional-order sir epidemic model for transmission prediction of covid-19 disease. *Appl. Sci.* **2020**, *10*, 8316.
26. Zhang, Y.; Wang, Y.; Wang, T.; et al. Stability and bifurcation analysis on a fractional model of disease spreading with different time delays. *Neural Process. Lett.* **2022**, *54*, 1977–1993.
27. Skwara, U.; Mozyrska, D.; Aguiar, M.; et al. Dynamics of vector-borne diseases through the lens of systems incorporating fractional-order derivatives. *Chaos Solit. Fractal.* **2024**, *181*, 114643.
28. Mandal, D.S.; Sha, A.; Chattopadhyay, J. Dynamical study of fractional order differential equations of predator-pest models. *Math. Methods Appl. Sci.* **2019**, *42*, 4225–4243.
29. Henriques, M.; Valério, D.; Gordo, P.; et al. Fractional-order colour image processing. *Mathematics* **2021**, *9*, 457.
30. Song, P.; Zhao, H.; Zhang, X. Dynamic analysis of a fractional order delayed predator-prey system with harvesting. *Theory Biosci.* **2016**, *135*, 59–72.
31. Owolabi, K.M. Mathematical modelling and analysis of two-component system with Caputo fractional derivative order. *Chaos Solit. Fractal.* **2017**, *103*, 544–554.
32. Chinnathambi, R.; Rihan, F.A. Stability of fractional-order prey-predator system with time-delay and Monod-Haldane functional response. *Nonlinear Dyn.* **2018**, *92*, 1637–1648.
33. Çelik, C.; Değerli, K. Hopf bifurcation analysis of a fractional-order Holling-Tanner predator-prey model with time delay. *The Anziam J.* **2022**, *64*, 23–39.
34. Baisad, K.; Moonchai, S. Analysis of stability and Hopf bifurcation in a fractional Gauss-type predator-prey model with Allee effect and Holling type-III functional response. *Adv. Differ. Equ.* **2018**, *2018*, 82.
35. Xu, C.; Mu, D.; Pan, Y.; et al. Exploring bifurcation in a fractional-order predator-prey system with mixed delays. *J. Appl. Anal. Comput.* **2023**, *13*, 1119–1136.
36. Alidousti, J. Stability and bifurcation analysis for a fractional prey-predator scavenger model. *Appl. Math. Modell.* **2020**, *81*, 342–355.
37. Li, Z.; Zhang, W.; Huang, C.; et al. Bifurcation for a fractional-order Lotka-Volterra predator-prey model with delay feedback control. *Aims Math.* **2021**, *6*, 675–687.
38. Podlubny, I. *Fractional Differential Equations*; Mathematics in Science and Engineering; Academic Press: San Diego, CA, USA, 1999.